




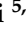


Article

Enviro-Economic Assessment of HHO–CNG Mixture Utilization in Spark Ignition Engine for Performance and Environmental Sustainability

Muhammad Usman ¹, Muhammad Ali Ijaz Malik ¹, Rehmat Bashir ¹, Fahid Riaz ²,
Muhammad Juniad Raza ³, Khubaib Suleman ³, Abd-ul Rehman ³, Waqar Muhammad Ashraf ^{4,*}
and Jaroslaw Krzywanski ^{5,*}

¹ Department of Mechanical Engineering, University of Engineering and Technology, GT Road, Lahore 54890, Pakistan

² Department of Mechanical Engineering, Abu Dhabi University, Abu Dhabi P.O. Box 59911, United Arab Emirates

³ Department of Mechanical Engineering, RCET University of Engineering and Technology, Gujranwala 43741, Pakistan

⁴ Centre for Process Systems Engineering, Department of Chemical Engineering, University College London, Torrington Place, London WC1E 7JE, UK

⁵ Faculty of Science and Technology, Jan Dlugosz University in Czestochowa, 42-200 Czestochowa, Poland

* Correspondence: waqar.ashraf.21@ucl.ac.uk (W.M.A.); j.krzywanski@ujd.edu.pl (J.K.)



Citation: Usman, M.; Malik, M.A.I.; Bashir, R.; Riaz, F.; Raza, M.J.; Suleman, K.; Rehman, A.-u.; Ashraf, W.M.; Krzywanski, J. Enviro-Economic Assessment of HHO–CNG Mixture Utilization in Spark Ignition Engine for Performance and Environmental Sustainability. *Energies* **2022**, *15*, 8253. <https://doi.org/10.3390/en15218253>

Academic Editor: Dimitrios C. Rakopoulos

Received: 29 September 2022

Accepted: 1 November 2022

Published: 4 November 2022

Publisher's Note: MDPI stays neutral with regard to jurisdictional claims in published maps and institutional affiliations.



Copyright: © 2022 by the authors. Licensee MDPI, Basel, Switzerland. This article is an open access article distributed under the terms and conditions of the Creative Commons Attribution (CC BY) license (<https://creativecommons.org/licenses/by/4.0/>).

Abstract: Road transportation has received the attention of researchers due to its higher carbon footprint. Alternative fuels present major advantages in terms of environmental sustainability. For this reason, an enviro-economic analysis of alternative fuels carries great significance. However, scarce attempts have been rendered in order to ascertain the impact of a hydroxy gas (HHO) and compressed natural gas (CNG) mixture on sustainable environmental development. The current study addresses this issue by employing an HHO–CNG mixture and gasoline in spark ignition (SI) engines for the purposes of performance and environmental pollutants measurement. Then, engine emission data were substituted for Weibull distribution in order to establish suitability for 50 and 95% confidence intervals (CIs). The mixture outperformed gasoline in terms of brake-specific fuel consumption (BSFC) and emission contents. On average, hydroxy gas with CNG produced 10.59% lower oxides of nitrogen (NO_x) comparative to gasoline. Finally, the enviro-economic analysis also turned out to be in favor of the hydroxy gas mixture owing to a saving of 36.14% in USD/year due to 27.87% lower production of carbon dioxide (CO₂) emission.

Keywords: renewable fuels; SI engine; Weibull distribution; enviro-economic analysis; CO₂ abatement; global warming

1. Introduction

Fossil fuels have been considered significant energy resources for many years, but they also yield many harmful pollutants. Therefore, the amount of these harmful pollutants keeps increasing in the environment, which has, subsequently, disturbed climatic balance and conditions [1]. The transport sector consumes 18% of the global primary energy and is responsible for 23% of global CO₂ emissions, which ultimately results in global warming [2,3]. The world is facing the utmost global issue of climate change owing to these extreme impacts to the ecosystem [4]. Conventional fossil fuels are consumed drastically, and their consumption increases by 19.6% due to the quest for a luxurious lifestyle [5]. The Energy Information Administration has stated that global energy consumption is approximated to increase by 56% in the year 2040 with reference to 2010 [6]. Fossil fuels have served as a major source of the total global primary energy mix, approximately 85% in 2001 and which raised to 90% by 2020 [7]. Almost all renewable fuels are environmentally

friendly as compared to conventional fossil fuels, but still, there are technical, economic, and social issues for their adoption as an alternative to fossil fuels. Hence, to avoid the emission of these unwanted gases, spark ignition (SI) engines are now being operated on alternative fuels, such as on liquified petroleum gas (LPG), CNG, and ethanol [8–10]. Alcohol-based fuels can also be a good alternative to gasoline due to their higher octane number, higher heat of vaporization, less volatility, and higher oxygen content; further, they can be manufactured sustainably from carbon-based feedstocks, but, it must be noted that, they have lower calorific values [11,12]. They have chemical properties similar to gasoline and require very little modification to use them in existing engines, they also come with a significant reduction in exhaust gases [13–15]. The main disadvantage of using alternative fuels is that they produce less power when compared to gasoline under the same condition of engines running [16,17].

Therefore, the focus of research has shifted to discovering renewable sources of energy in order to simultaneously achieve brake power (BP) along with minimizing the emission of unwanted harmful gases to meet the power requirement that is already in place and to enhance environmental safety. The robust nature of hydrogen and the complexities in its storage limit its use in automobiles. Therefore, scientists are focusing on hydroxy gas (HHO), as it can be produced through an onboard hydrogen generation system [18]. Hydroxy gas (HHO) is a mixture of hydrogen gas and oxygen gas in molar (or volume) ratio 2:1. It means that HHO gas is composed of a 11% mass of molecular hydrogen and a 89 mass% of molecular oxygen. HHO is a potential candidate as a renewable fuel, which can be used in a mixture with other fuels, such as CNG to bridge the power gap in SI engines when operated solely on these fuels [19–23]. HHO can be considered a renewable fuel as it is produced directly from the electrolysis of water, and water is renewable in nature in terms of its natural existence. Moreover, HHO has no carbon, and as a result its carbon footprint is zero, which can help the reduction in carbon emissions. Hydroxy gas provides clean burning when compared to coal and fossil fuels. In addition, it is not as controversial as nuclear energy and it still limits the greenhouse effect [24,25]. Hydroxy gas (HHO) can be formed by separating the atoms of the water molecule through electrolysis (theoretically 67% vol. H_2 and 33% vol. O_2) [26]. Further, its calorific value is extremely high with respect to diesel and gasoline. The calorific value of 1 kg of HHO is 3 and 3.2 times greater than gasoline and diesel fuel, respectively [27]. A comparative analysis of using HHO–CNG blends was performed in a gasoline-fueled engine, which showed comparable results for engine performance with regard to gasoline [28]. Moreover, a significant reduction in exhaust emission gases was also observed [29]. Both CNG and HHO can produce a different impact on combustion properties when compared to gasoline due to their different physicochemical properties [30].

Usman et al. [31] found that the brake power (BP) produced by the engine in the case of gasoline was 28.8% higher than that of CNG, however this came with the cost of a 17.2% higher fuel consumption. In another study, they [32] found that the brake power produced by the engine in the case of CNG was 26.4% lower than gasoline, but the mixing of HHO with CNG helped to regain the brake power by 11.28%. The brake-specific fuel consumption (BSFC) in the case of HHO–CNG was 31.1 and 16.9% lower than gasoline and CNG, respectively. Musmar and Rousan [33] investigated the impact of hydroxy gas (HHO) on a 197 cc single-cylinder SI engine. They found up to a 40% reduction in hydrocarbon (HC) and CO_2 emissions. In addition, the carbon monoxide (CO) and NO_x emissions decreased by 20 and 54%, respectively. Farooq et al. [34] investigated the performance and emissions of SI engines fueled with CNG and a HHO–CNG mixture. They found that brake power decreased for CNG, but the engine's brake thermal efficiency (BTE) significantly improved. Likewise, CNG's CO, HC, and CO_2 emissions declined, but NO_x emissions increased. However, the addition of HHO with CNG improved the brake power at the cost of lower fuel consumption and increased brake thermal efficiency (BTE). The HC, NO_x , CO_2 , and CO emissions also reduced for the HHO–CNG mixture. They concluded that the HHO–CNG mixture is not only beneficial in terms of engine performance but is also

eco-friendly. Wang et al. [35] investigated the impact of a 3% HHO blend with gasoline on engine performance and emissions. They found a decline in CO and HC emissions but a rise in NO_x emissions. They observed higher flame speed in the case of HHO-blended fuel, which is mainly responsible for reducing heat losses with improvements in BTE and ultimately a better combustion, which is responsible for the higher NO_x output.

Consequently, the combination of HHO and CNG in an SI engine may produce a prominent impact on engine performance. The existing literature needs to be upgraded by unveiling the enviro-economic impact of these alternatives in order to describe the changes in engine performance along with exhaust emissions. Therefore, HHO–CNG should be examined as an alternative fuel in SI engines. In the present study, the gradual increment in engine rpm is made with the aim of measuring brake power (BP), exhaust gas temperature (EGT), exhaust emissions (HC, NO_x, CO, and CO₂) and brake-specific fuel consumption (BSFC). In addition, the engine emission levels data were substituted for Weibull distribution in order to establish suitability for 50% and 95% confidence intervals. Finally, enviro-economic analysis was performed on CO₂ emission in order to identify the deterioration impact on the environment and tax imposition cost. A comparative assessment based on engine performance and exhaust emissions from the engine was performed between the various gaseous fuel options, i.e., a HHO–CNG blend, CNG alone, and liquid fuel (i.e., gasoline).

2. Materials and Methods

In this study, a HHO–CNG blend and gasoline are investigated in how they affect the performance and exhaust emissions of the SI engine (the specifications of which are given in Table 1).

Table 1. Attributes of the 4-stroke heat engine.

Engine Parameters	Specification
Number of cylinders	1
Capacity (cc)	219
Cooling system	Water cooled
Peak torque (Nm)	15.1
Ignition type	Spark aided
Peak power (kW)	7.4
Bore and stroke (mm)	67 × 62.2

2.1. Schematic Arrangement

A schematic arrangement of all the auxiliary and testing instruments attached to the engine is shown in Figure 1. Torque was ascertained through a dynamometer (7 inch kart, dynamite) according to the SAE standard (J1349). The water brake dynamometer was connected to the shaft of the engine. The dynamometer is composed of toroidal pockets such that these pockets are driven by the engine. The load on the engine was applied through a supply of water from one horsepower motor. The water pressure was controlled by the load control valve. The water, when struck with the toroidal pockets, then was whipped around them; further, the shear forces in the water acted tangential to the housing radius and acted as the load on the engine. A thermocouple (K-type) was inserted in the exhaust pipe in order to measure the exhaust gas temperature (EGT). The thermal and physicochemical attributes of all three fuels, i.e., CNG, HHO, and gasoline, are described in Table 2. Gasoline was fueled into the engine through a carburetor, while a CNG kit was used in order to maintain the supply of CNG at 1.1 bar. The crossover kit contains two valves, one for safety purposes and the other to regulate the gas pressure about 1.1 bar higher than the pressure at the intake manifold. The CNG at 1.1 bar and HHO at 10 scfh were supplied separately to the engine in order for it to burn as an HHO–CNG blend. The

HHO unit comprised a cathode and anode that was dipped in the electrolyte in order to produce hydroxy gas through the following electrolytic reaction [36].

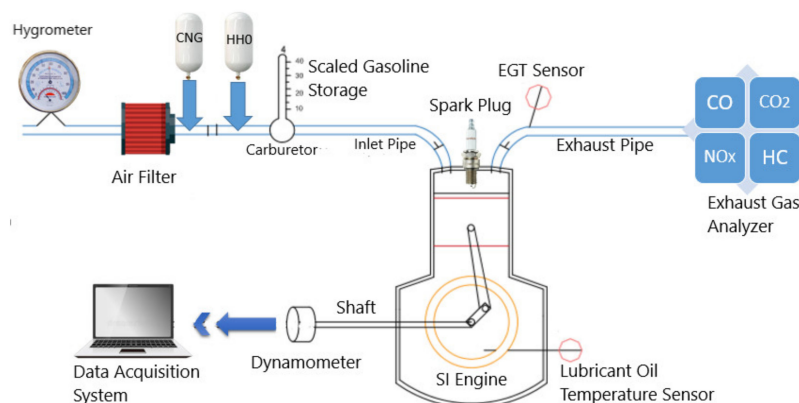
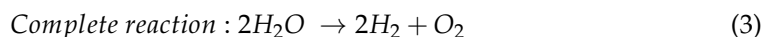
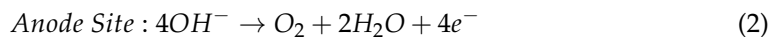
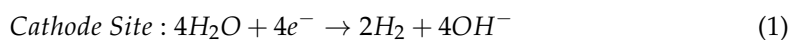


Figure 1. Experimental setup.

Table 2. Physiochemical attributes of fuels ^c.

Properties	HHO	CNG	Gasoline
Phase	Gas	Compressed gas	Liquid
RON ^a	>130	120	97
Density (kg/liter at 15.48 °C)	0.0827 ^b	0.128	0.73
Air to fuel ration (A/F)	34.2	17	14.7
Ignition temperature (K)	867	723	633
Heating value (kJ/kg × 10 ³)	120	49	46.3

Abbreviations—RON: ^a Research octane number; ^b density in kg/m³ at 0 °C and 1 atm. ^c PSO: Pakistan state oil.

HHO was generated from a simple electrolytic cell, which possessed the dimensions of $16.5 \times 16.5 \times 0.1 \text{ cm}^3$ with an input voltage of about 35 V and input current of about 0–60 A while possessing 24 stainless-steel plates (316 L) with 2 mm spacing between them. The reactor comprised two anode plates located at the center portion with a seal, while two cathode plates located at both ends and the mass-by-volume mixture of 6 gram/liters of potassium hydroxide (KOH) and distilled waters were used as a catalyst [37]. HHO is produced through the electrolysis of water in an electrolytic cell, as mentioned above. At the cathode, water decomposed to hydrogen (H₂) and hydroxide (OH⁻) ions, as depicted in Equation (1). While at the anode, hydroxide ions decomposed to produce oxygen and water molecules, as shown in Equation (2). In the overall reaction (Equation (3)), the water molecules produce hydroxy gas (HHO). The probe of the exhaust gas analyzer (Testo-350) is introduced into the exhaust pipe of an engine in order to measure the emissions of NO_x, CO₂, CO, and HC.

2.2. Test Approach

Initially, the calibration was conducted for each test as per the recommendations of the manufacturer. Afterwards, BP, BSFC, and EGT were analyzed at eight different speeds for two test runs. The comprehensive experimental plan is displayed in Table 3. A fuel delivery system with a transparent measuring cylinder was used in order to monitor the fuel consumption of gasoline, while a digital weight measuring machine was utilized to observe the consumption rate of CNG. The flow rate of HHO was gauged by the gas

rotameter, which was installed at the outlet of the HHO unit. Table 3 shows the variation in engine rpms used to quantify the exhaust gas emissions in the case of the HHO–CNG blend and gasoline. The accuracy of emission levels was analyzed through Weibull distribution for 50% and 95% CIs. The probe of Testo-350 was inserted into the exhaust duct for one minute at a distinct engine speed (rpm) in order to obtain stability in the readings. The measurement range and accuracy of the emission analyzer (Testo-350) for each emission parameter is detailed in Table 4.

Table 3. Comprehensive empirical strategy.

Factors	Divisions
Speed range	1600 to 4400 rpm with gap of 400 rpm
Throttling	80% wide open throttle (WOT) condition
Fuel	CNG, HHO–CNG, and gasoline
Performance parameters	BP, BSFC, and EGT
Emission parameters	CO, CO ₂ , HC, and NO _x
Statistical tool	Weibull distribution for 50% and 95% confidence intervals

Table 4. Measurement Range and Accuracy of Testo-350.

Emission Parameters	Measurement Range	Accuracy
CO	0–10,000 ppm	±5 ppm
NO _x	0–4000 ppm	±1 ppm
HC	100–18,000 ppm	±2% of reading
CO ₂	0–50%	±0.3%

2.3. Environmental and Enviro-Economic Assessment

Environmental and enviro-economic analyses have been performed on a 219cc gasoline engine. The Paris Conference on Climate Change (2015) revealed that CO₂ concentration can be reduced by the capture and storage of CO₂ [38]. In this study, the methods developed by Caliskan in 2017 [39] were applied. Further, certain norms were applied before the environmental and enviro-economic analyses, such as the Engine being operated 8 h a day, and then extrapolated for the whole year (which turns out to be 2920 h). For the environmental analysis of the fuels, the following equation, as proposed by Caliskan, was applied.

$$X_{CO_2} = Y_{CO_2} \times W_{gen} \times t_{working}$$

where Y_{CO_2} = the mass of carbon dioxide, in grams, that is produced when an engine generates the energy of 1 kWh (g CO₂/kWh); W_{gen} = power output of the engine at a particular rpm, $t_{working}$ = the working time, in hours, for a year (h/yr); and X_{CO_2} = the mass of carbon dioxide per year (t CO₂/yr).

We accounted for the economic aspect of CO₂ in the analysis. This was done due to the fact that the emissions play an important role in understanding the impact of global warming on the economy. Carbon prices are variable and vary from country to country, as such this must be understood in order to meet the aim of reducing global warming. The price of Swiss carbon is used as a basis in order to calculate the cost of carbon in the context of European countries. The price of Swiss carbon is estimated to be 8.28 USD/t CO₂ [40].

3. Results

The comparative assessment of the HHO–CNG blend and gasoline fuel showed relative improvement in engine performance and control of emissions when the HHO–CNG blend was used as the main fuel.

3.1. Comparative Performance Assessment

The comparative assessment of the two test fuels based on brake power (BP) is shown in Figure 2a, which demonstrates a comparatively high BP that is produced in the case

of gasoline, in a specified range of rpm. On average, BP generated by the HHO–CNG mixture was 14.81% lower when compared to gasoline (G_{97}). Lower air displacement and flame velocity are two main reasons for the decline in brake power, as is in the case of CNG. The amount of suction air remains the same for gasoline as described in [31,41], while air is replaced by gaseous fuels resulting in a lower energy density when compared to liquid fuel. Therefore, there should be a significant decrease in brake power when using CNG for an engine that is designed to be powered by gasoline. However, when a mixture of hydroxy gas (HHO) and CNG is used, the brake power increases due to the presence of HHO, which has a higher heating value compared to CNG alone [42]. Figure 2c depicts variation in EGT at various engine rpm, such that a higher value of temperature for gasoline within the whole range of rpm is observed when compared to gaseous fuel. A relative decrease of 4.78% in the value of exhaust gas temperature was observed for the HHO–CNG mixture. The decline in EGT and BP for gaseous fuel can be credited to an unaltered ignition timing [31]. Moreover, more fuel consumption in the case of liquid fuel is mainly responsible for more fuel burning and higher exhaust gas temperatures. Figure 2b depicts the comparison between gaseous and liquid fuels at various different speeds based on BSFC. Further, the gasoline had augmented BSFC when compared to the HHO–CNG mixture throughout the engine rpm range. The higher calorific value of the HHO–CNG mixture when compared to gasoline reduced the value of BSFC by 32.30% as described in [25,43]. However, all fuels have a similar trend for variation in BSFC at different engine speeds, i.e., first they decline then rise, as speed increases. The possible reason for the higher value of BSFC may be due to the increased heat loss at low engine speed and a relatively higher increase in friction at high engine speed [44].

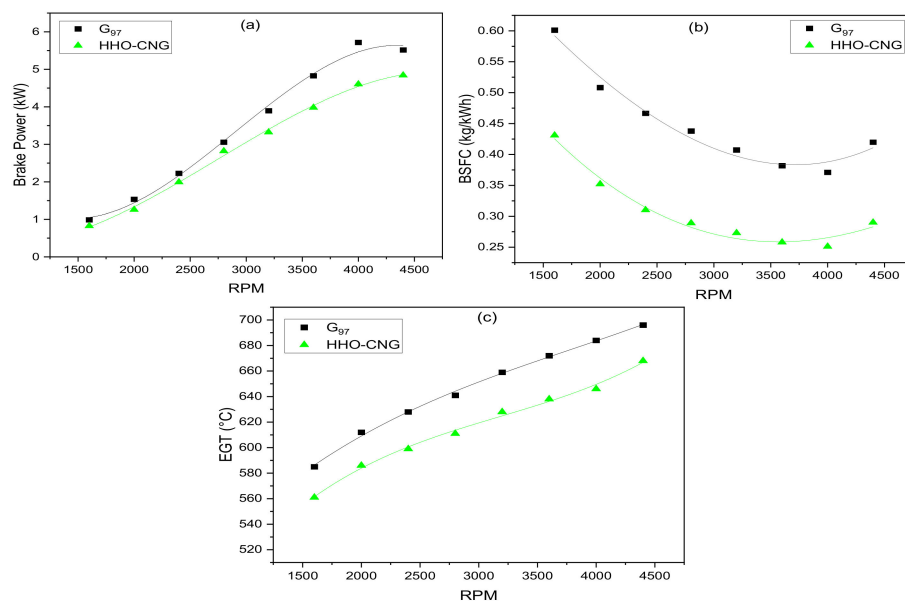


Figure 2. (a) BP, (b) BSFC, and (c) EGT for gasoline and HHO–CNG.

3.2. Exhaust Emissions

The comparison of engine emissions for both fuels is shown in Figures 3–6. It is evident from Figure 3 that the HHO–CNG blend produced less HC emission as compared to gasoline, as the average HC emission concentrations were 1396.5 ppm and 622.88 ppm for gasoline and HHO–CNG, respectively, as shown in Table 5.

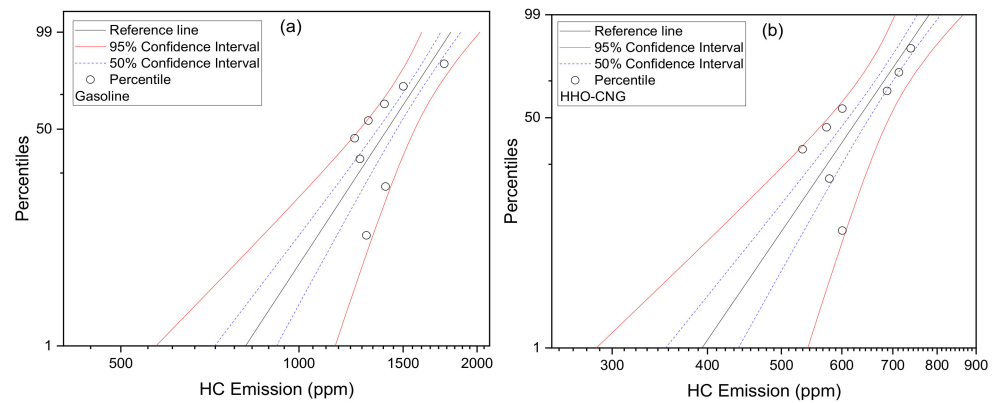


Figure 3. (a) HC Weibull distributions for various CIs using gasoline and (b) HC Weibull distributions for various CIs using HHO-CNG.

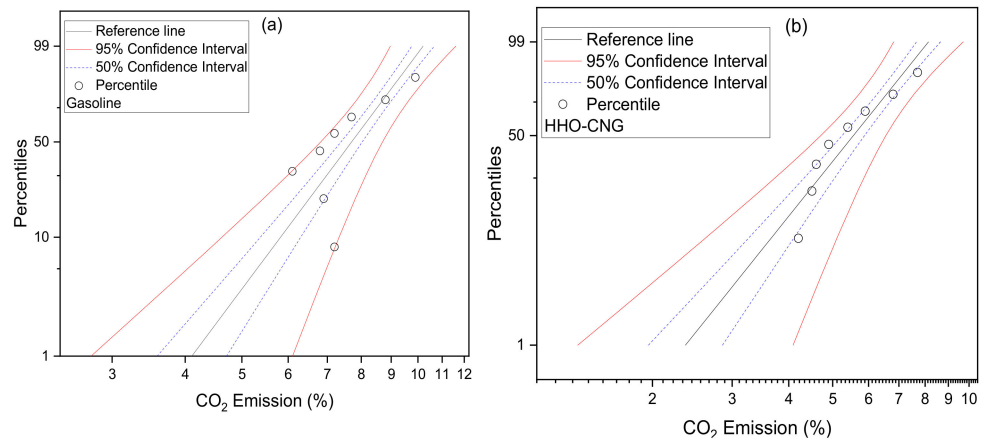


Figure 4. (a) CO₂ Weibull distributions for various CIs using gasoline and (b) CO₂ Weibull distributions for various CIs using HHO-CNG.

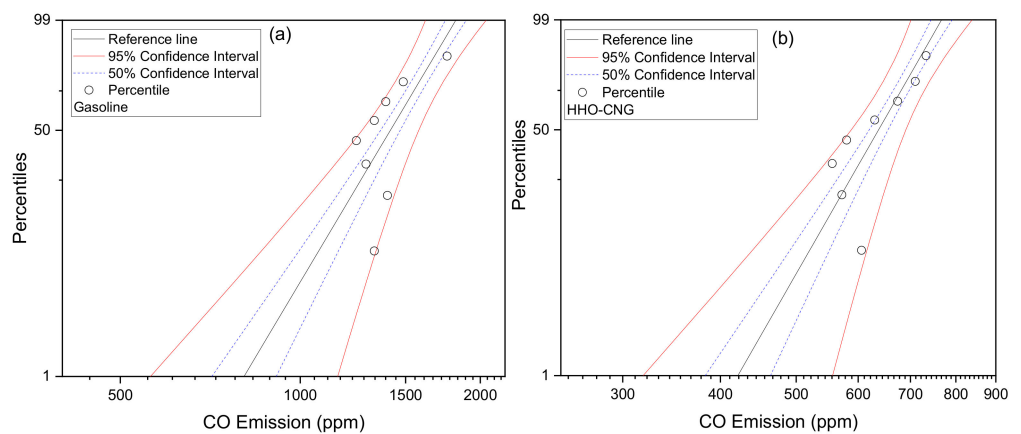


Figure 5. (a) CO Weibull distributions for various CIs using gasoline and (b) CO Weibull distributions for various CIs using HHO-CNG.

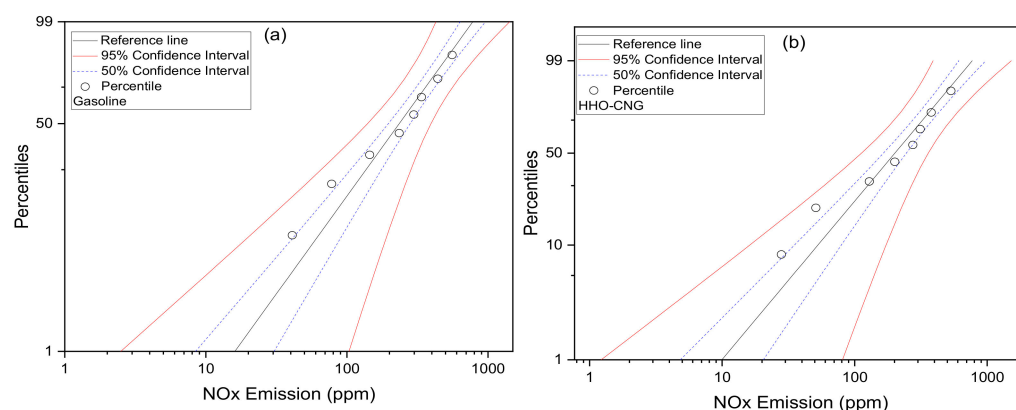


Figure 6. (a) NO_x Weibull distributions for various CIs using gasoline and (b) NO_x Weibull distributions for various CIs using HHO–CNG.

Table 5. Average HC emission contents for 50% and 95% confidence intervals.

Fuel Type	HC Emission Content (ppm)				
	Mean ± Stdev	<i>p</i> Value	Skewness	Mean ± 50% CI	Mean ± 95% CI
Gasoline	1396.5 ± 194.02	>0.25	0.95	1396.5 ± 46.27	1396.5 ± 134.54
HHO–CNG	622.88 ± 85.20	>0.25	0.0077	622.88 ± 20.32	622.88 ± 59.05

Homogenous mixing of liquid fuel in the air requires more time due to its prior atomization and then vaporization, which is not required in the case of gaseous fuels. This better mixing of gaseous fuels, and their lower molecular weight, leads to the appropriate air–fuel mixture burning, which, consequently, results in less HC content [45,46].

CO₂ emission content is represented in Figure 4, which shows the lower CO₂ for the HHO–CNG mixture as compared to gasoline. Table 6 shows the average content of CO₂ emission, and Figure 4 describes the CO₂ emission distribution for both fuels. HHO–CNG mixture produced lower CO₂ content than gasoline.

Table 6. Average CO₂ emission contents for 50% and 95% confidence intervals.

Fuel	Carbon Dioxide Emission Content (CO ₂ %)				
	Mean ± Stdev	<i>p</i> Value	Skewness	Mean ± 50% CI	Mean ± 95% CI
Gasoline	7.62 ± 1.21	>0.25	0.95	7.62 ± 0.29	7.62 ± 0.84
HHO–CNG	5.5 ± 1.23	>0.25	0.90	5.5 ± 0.29	5.5 ± 0.85

HHO–CNG showed a relative decrease of 27.87% in the contents of CO₂ when compared to gasoline. The major cause for the decline in CO₂ emissions is the lower proportion of carbon atoms that are present in gaseous fuels when compared to liquid [47]. The distribution of carbon contents is illustrated in Figure 5. CO is present in exhaust emissions as a result of incomplete combustion [48]. Table 7 shows the CO emissions in the case of both fuels.

Table 7. Average CO emission contents for 50% and 95% confidence intervals.

Fuel	Carbon Monoxide Emission Content (CO ppm)				
	Mean ± Stdev	<i>p</i> Value	Skewness	Mean ± 50% CI	Mean ± 95% CI
Gasoline	1399.25 ± 202.74	>0.25	0.84	1399.25 ± 48.35	1399.25 ± 140.49
HHO–CNG	628.88 ± 76.3	>0.25	−0.085	628.88 ± 18.08	628.88 ± 52.53

A relative decrease of 55.05% in CO contents was observed for the HHO–CNG mixture. Figure 6 shows the distribution of NO_x emissions for liquid and gaseous fuels. Table 8

describes the average NO_x emission contents of the 266.63 ppm and 238.38 ppm produced by gasoline and the HHO–CNG blend, respectively. These results are similar to those of the exhaust gas temperature for test fuels under similar conditions. NO_x is primarily produced from the reaction between oxygen and nitrogen in a combustion chamber under high-temperature conditions [25,31,49]. It can be realized from emission data that *p*-values characterize a high level of significance.

Table 8. Average NO_x emission contents for 50 and 95% confidence intervals.

Fuel	Oxides of Nitrogen Emission Contents (NO _x _ ppm)				
	Mean ± Stdev	<i>p</i> Value	Skewness	Mean ± 50% CI	Mean ± 95% CI
Gasoline	266.63 ± 178.52	>0.25	0.34	266.63 ± 42.57	266.63 ± 123.70
HHO–CNG	238.38 ± 171.46	>0.25	0.43	238.38 ± 40.89	238.38 ± 118.81

The exhaust emissions from the engine, including the HC, CO₂, CO, and NO_x produced by gasoline and the HHO–CNG blend fuels with 50% and 95% confidence intervals (CIs), are analyzed in the form of probability plots through a Weibull distribution, which are shown in Figures 3–6. The adequacy of emission data for two types of fuel were examined for the confidence intervals (CIs) of 50% and 95% CIs and the obtained Weibull distributions were observed as encapsulated within the confidence intervals (CIs). The most excellent fit was observed by the Weibull distribution fit, around the middle of the Weibull distribution, with the absence of a heavy tail at the upper segment of the distribution. It can be observed from Figures 3a–6a that HC, CO₂, CO, and NO_x exhaust emissions distribution for gasoline fit well within the 50% and 95% CIs, respectively. Similarly, Figures 3b–6b depict good agreement with the Weibull distribution of emission levels of HC, CO₂, CO, and NO_x when the engine is fueled with HHO–CNG for 50% and 95% confidence intervals (CIs), respectively.

With eight CO emission data points, HHO–CNG data were located near the reference line in contrast with data points of liquid fuel and showed less variability. For gasoline, the 95% confidence interval for the 50th percentile of carbon monoxide datapoints distribution ranges between 1268.41 and 1577.81 ppm (Figure 5a). Moreover, the mean of the CO datapoints distribution produced by gasoline, shows that it has a 50% confidence interval (CI) range between 1362.53 and 1468.82 ppm (Figure 5a). Likewise, for HHO–CNG fuel, the 95% confidence interval (CI) and 50% CI for the 50th percentile of CO datapoints distribution ranges between 588.16 to 690.57 ppm and 619.95 to 655.16 ppm, respectively (Figure 5b).

Out of many significant attributes of the CIs, the major significant attribute of them is that the average values of any dataset need not be symmetric. For the eight emission levels data set, the positively skewed distribution was obtained for gasoline, and the negatively skewed distribution was obtained for HHO–CNG (see Table 6). The positively skewed distribution indicates that the tail on the right side of the distribution is longer. While the negatively skewed indicates that the tail on the left side of the distribution is longer, and, ultimately, an unsymmetric distribution is obtained.

In addition, the moderately skewed distributions were found to exclude the heavily skewed hydrocarbon distributions employing gasoline and the HHO–CNG blend (Figure 3a,b). Moreover, the asymmetric confidence intervals were obtained, on average, because of positively skewed confidence intervals. In regard to CO₂ emission, a positively skewed distribution was found for both gasoline and HHO–CNG. For gasoline, the 95% confidence interval for the 50th percentile of carbon dioxide emission distribution ranges between 6.82 and 8.69% (Figure 4a). Moreover, the mean CO₂ emission distribution produced by gasoline, having a 50% confidence interval (CI), ranges from 7.39 to 8.03% (Figure 4a). Likewise, for the HHO–CNG fuel, in regard to the 95% confidence interval (CI) and 50% CI (for the 50th percentile of CO₂ emission) distribution ranges from 4.71 to 6.55% and 5.25 to 5.88%, respectively (Figure 4b).

The positive skewness in NO_x emission data for HHO–CNG indicate a more unsymmetric nature of distribution and more of an inclination of the tail toward the right side. For gasoline, the 50th percentile under 95% CI of nitrogen oxide (NO_x) emission distribution ranges from 139.97 to 394.32 ppm (Figure 6a). Moreover, the mean NO_x emission distribution produced by gasoline, having a 50% confidence interval (CI), ranges from 196.58 to 280.76 ppm (Figure 6a). Likewise, for HHO–CNG fuel, the 95% confidence interval (CI) and 50% CI for the 50th percentile of CO₂ emission distribution ranges from 112.58 to 358.79 ppm and 164.64 to 245.34 ppm, respectively (Figure 6b).

3.3. Enviro-Economic Assessment

For the purposes of enviro-economic analysis, a single-cylinder SI engine fueled with gasoline (G₉₇) and HHO–CNG fuel was examined at a 80% WOT condition via varying speeds from 1600 to 4400 rpm, based on experimental emissions data. In the framework of the design of the experiment, the CO₂, CO, HC, and NO_x were measured quantities. The relation between CO₂ emission with engine speed along with cost variation is displayed in Figure 7. It can be clearly seen from Figure 7a that the HHO–CNG mixture produced a lower CO₂ content when compared to G₉₇. About a 27.87% reduction in CO₂ content was observed for the HHO–CNG mixture in contrast to G₉₇. On average, gasoline and HHO–CNG produced 483.96 and 349.09 g/kWh of CO₂ emissions, respectively. The lower carbon content in HHO–CNG [47] and the better combustion owing to hydroxy gas presence are mainly responsible for the reduction in CO₂ emissions. The existence of hydrogen (H₂) in the HHO mixture may induce a burning temperature and OH- radical concentration, which is ultimately responsible for an improved oxidation process inside the combustion chamber [50]. Figure 7b reveals the calculation results of enviro-economic analyses. It can be clearly seen that CO₂ emission exhibits a linear relationship with engine speed. Both gasoline and HHO–CNG produced the least CO₂ emission at the lowest speed (1600 rpm) of 0.15 and 0.07 ton/year. The maximum CO₂ emissions of 0.77 ton/year and 1.12 ton/year were achieved at 4400 rpm for HHO–CNG and gasoline, respectively. The associated economic cost with CO₂ emission at 4400 rpm is 6.34 and 9.29 USD/year for HHO–CNG and gasoline fuel. On average, the HHO–CNG mixture is responsible for a 36.14% decline in economic cost associated with CO₂ emission, in comparison with gasoline. According to the International Energy Agency, alongside other activities [51–57], the presented considerations are in line with Net Zero Emissions according to the 2050 scenario [58].

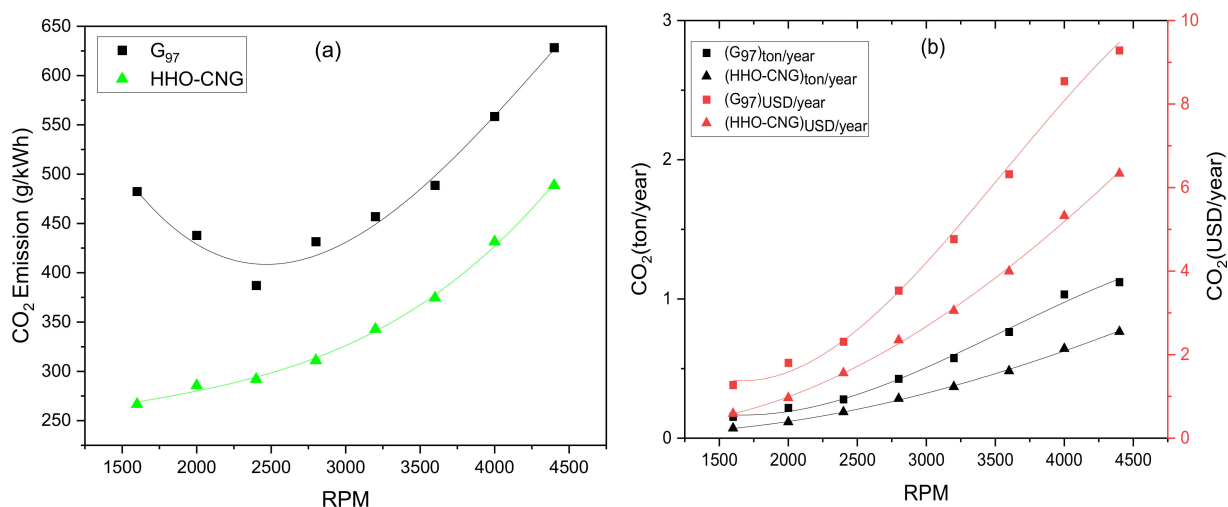


Figure 7. (a) CO₂ emission variations with respect to engine speed in terms of percentage by volume and (b) CO₂ emission variations in terms of ton/year when associated with cost variation for a year against engine speed.

Figure 8 demonstrates the variation in CO content with respect to engine speed. The CO content exhibit a directly proportional relation with incomplete combustion; this is because CO content increases owing to incomplete combustion [48]. Therefore, the apparent decrease in CO content can be seen for HHO–CNG in contrast with G₉₇. On average, a 55.05% decline in CO content was obtained for the HHO–CNG mixture when compared to G₉₇. This decline in CO₂ and CO concentrations for the HHO–CNG mixture is due to a higher H/C ratio. The mixture with lower carbon content produces lower carbon-oxygen reaction fractions in the exhaust [59]. Additionally, the lean working states of the engine due to hydroxy gas and improved combustion, played their role in lowering CO contents [15]. Both gasoline and HHO–CNG produced the least CO emission at the lowest speed (1600 rpm) of 0.0018 and 0.0006 ton/year. The maximum CO emissions of 0.0041 ton/year and 0.0112 ton/year were achieved at 4400 rpm for HHO–CNG and gasoline, respectively. On average, gasoline and HHO–CNG produced 5.02 and 2.26 g/kWh of CO emission, respectively.

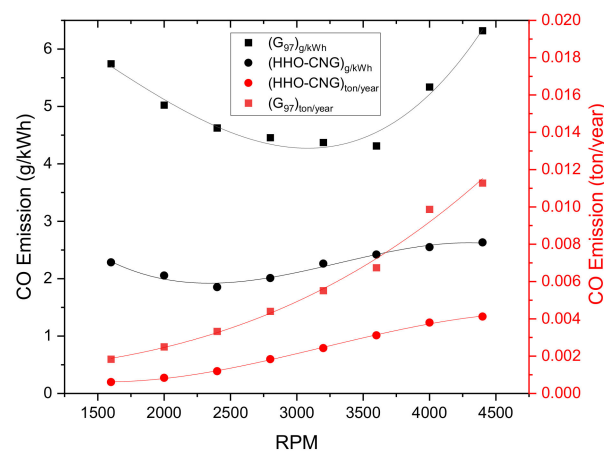


Figure 8. CO emission variation with respect to engine speed in terms of parts per million and ton/year.

Figure 9 depicts the variation in HC emissions from engine fueled with gasoline and the HHO–CNG blend. The gaseous fuel (HHO–CNG) produced lower HC content over eight engine speeds. On average, gasoline and HHO–CNG produced 2.80 and 1.25 g/kWh of HC emission, respectively. HC emission increases with the increment in engine speed. The highest HC emission in the case of gasoline and HHO–CNG were 0.0063 and 0.0023 ton/year, respectively, at 4400 rpm. The fuel in gaseous form undergoes appropriate mixing with air during intake, but fuel in the liquid form first undergoes atomization and then undergoes vaporization following the homogeneous mixing with air during the intake stroke, which consumes more time. Therefore, gaseous fuels produced a better mixture formation [45]. Furthermore, the molecular weight of CNG and HHO is lower when compared to gasoline, which is mainly responsible for efficient fuel burning. All these reasons are majorly responsible for lower HC emissions in the case of the HHO–CNG mixture. The results showed that the HC emission significantly declines for HHO–CNG fuel in comparison with gasoline. About a 55.39% decline in average HC content was obtained for HHO–CNG in contrast with gasoline. The better fuel mixing at intake, owing to the gaseous nature of HHO and CNG, significantly reduces HC emission, which, consequently, reduces the adsorption and desorption of fuel particles in lubricant oil film [60].

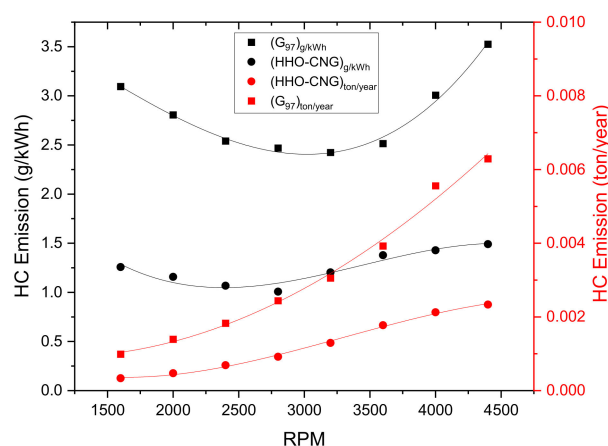


Figure 9. HC emission variation with respect to engine speed in terms of parts per million and ton/year.

Figure 10 displays the variation in NOx emissions for both fuels under eight different engine speeds. It is prominently seen that gasoline produced more NOx emissions than the HHO–CNG blend. The NOx contents for two test fuels were in accordance with the EGT behavior for these fuels. The amount of air during suction and in-cylinder combustion is mainly responsible for NOx emission. NOx emission augments with the increase in the incoming air amount. The in-cylinder temperature rises with the progression in engine speeds owing to a relatively higher fuel consumption rate (more combustion). The higher the in-cylinder temperature, the higher the EGT will be [45,59]. It can also be concluded that owing to a higher temperature, nitrogen, and oxygen are readily available in the mixture to form NOx [49]. The NOx emission content increases with the engine speed. As the highest NOx emission in terms of ton/year obtained at maximum engine speed. The HHO–CNG blend produced 10.59% lower average NOx than gasoline. CNG and HHO replace air during intake owing to their gaseous nature, consequently reducing NOx emission. Moreover, the decline in NOx emission for the HHO–CNG blend in contrast with gasoline can also be credited to unchanged ignition timing [45]. On average, gasoline and HHO–CNG produced 1.77 and 1.58 g/kWh of NOx emission, respectively.

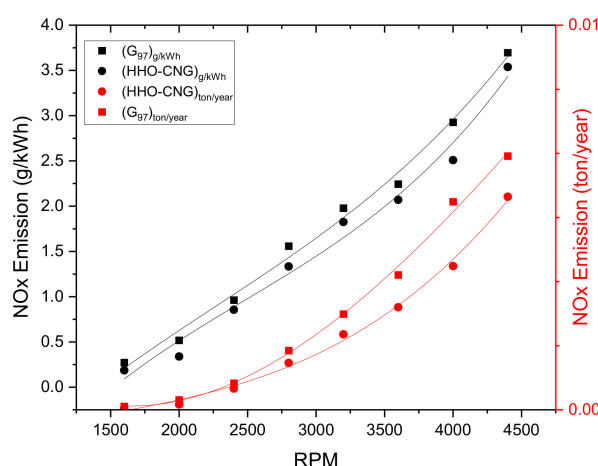


Figure 10. NOx emission variation with respect to engine speed in terms of parts per million and ton/year.

4. Conclusions

In this study, gaseous and liquid fuels were investigated to measure engine performance and exhaust emissions along with enviro-economic analysis. The results showed that gasoline produced 14.81% more brake power than the HHO–CNG blend. However, a

4.78% decrease in EGT takes place for the HHO–CNG mixture. The BSFC also declined by 32.30% for the HHO–CNG mixture in comparison with gasoline. Moreover, a significant decrease in emission contents of HC (55.39%), CO (55.05%) and CO₂ (27.87%) NO_x (10.59%) was observed for the HHO–CNG blend relatively to gasoline. Hence, the HHO–CNG blend is a more appropriate choice as an alternative fuel as compared to gasoline which not only produces lower harmful emissions but also produces significant power at the cost of lower energy input. Moreover, the associated economic cost with CO₂ emission at 4400 rpm is 6.34 and 9.29 USD/year for HHO–CNG and gasoline fuel. On average, the HHO–CNG mixture is responsible for a 36.14% decline in economic cost associated with CO₂ emission in comparison with gasoline. The mixture limit has been considered a safe limit to be used in the engine without any significant modification. In the future, excessive durability testing of the engine should be conducted for higher percentages of HHO in CNG in order to reduce the power gap and emission contents.

Author Contributions: Conceptualization, M.U. and M.A.I.M.; methodology, R.B.; software, F.R.; validation, M.J.R., K.S. and A.-u.R.; formal analysis, M.A.I.M. and J.K.; investigation, M.J.R.; resources, M.U. and W.M.A.; data curation, K.S.; writing—original draft preparation, F.R.; writing—review and editing, R.B., W.M.A. and J.K.; visualization, M.U. All authors have read and agreed to the published version of the manuscript.

Funding: This research received no external funding.

Conflicts of Interest: The authors declare no conflict of interest.

References

1. Ijaz Malik, M.A.; Usman, M.; Hayat, N.; Zubair, S.W.H.; Bashir, R.; Ahmed, E. Experimental evaluation of methanol-gasoline fuel blend on performance, emissions and lubricant oil deterioration in SI engine. *Adv. Mech. Eng.* **2021**, *13*, 16878140211025213. [CrossRef]
2. Demirbas, A.; Bafail, A.; Ahmad, W.; Sheikh, M. Biodiesel production from non-edible plant oils. *Energy Explor. Exploit.* **2016**, *34*, 290–318. [CrossRef]
3. Balat, H.; Öz, C. Technical and Economic Aspects of Carbon Capture and Storage—A Review. *Energy Explor. Exploit.* **2007**, *25*, 357–392. [CrossRef]
4. Iodice, P.; Senatore, A. Influence of Ethanol-Gasoline Blended Fuels on Cold Start Emissions of a Four-Stroke Motorcycle. Methodology and Results. 0148-7191; SAE Technical Paper; 2013. Available online: <https://pubmed.ncbi.nlm.nih.gov/15923082/> (accessed on 31 August 2021).
5. Singh, M.; Gandhi, S.K.; Mahla, S.K.; Sandhu, S.S. Experimental investigations on performance and emission characteristics of variable speed multi-cylinder compression ignition engine using Diesel/Argemone biodiesel blends. *Energy Explor. Exploit.* **2018**, *36*, 535–555. [CrossRef]
6. Malik, M.A.I.; Usman, M.; Bashir, R.; Hanif, M.S.; Zubair, S.W.H. Use of methanol-gasoline blend: A comparison of SI engine characteristics and lubricant oil condition. *J. Chin. Inst. Eng.* **2022**, *45*, 402–412. [CrossRef]
7. Balat, M. Usage of energy sources and environmental problems. *Energy Explor. Exploit.* **2005**, *23*, 141–167. [CrossRef]
8. Park, C.; Kim, C.; Lee, S.; Lee, S.; Lee, J. Comparative evaluation of performance and emissions of CNG engine for heavy-duty vehicles fueled with various caloric natural gases. *Energy* **2019**, *174*, 1–9. [CrossRef]
9. Alexander, J.; Porpatham, E. Investigations on Combustion Characteristics of Lean Burn SI Engine Fuelled with Ethanol and LPG. In Proceedings of the IOP Conference Series: Earth and Environmental Science, Malang City, Indonesia, 12–13 March 2019; p. 012020.
10. Rahman, M.A. Induction of hydrogen, hydroxy, and LPG with ethanol in a common SI engine: A comparison of performance and emission characteristics. *Environ. Sci. Pollut. Res.* **2019**, *26*, 3033–3040. [CrossRef]
11. Demirbas, A. Alternative fuels for transportation. *Energy Explor. Exploit.* **2006**, *24*, 45–54. [CrossRef]
12. Ozsezen, A.N.; Turkan, A.; Sayin, C.; Canakci, M. Comparison of performance and combustion parameters in a heavy-duty diesel engine fueled with iso-butanol/diesel fuel blends. *Energy Explor. Exploit.* **2011**, *29*, 525–541. [CrossRef]
13. Zhu, L.; He, Z.; Xu, Z.; Lu, X.; Fang, J.; Zhang, W.; Huang, Z. In-cylinder thermochemical fuel reforming (TFR) in a spark-ignition natural gas engine. *Proc. Combust. Inst.* **2017**, *36*, 3487–3497. [CrossRef]
14. Liu, J.; Duan, X.; Yuan, Z.; Liu, Q.; Tang, Q. Experimental study on the performance, combustion and emission characteristics of a high compression ratio heavy-duty spark-ignition engine fuelled with liquefied methane gas and hydrogen blend. *Appl. Therm. Eng.* **2017**, *124*, 585–594. [CrossRef]
15. Alrazen, H.A.; Ahmad, K. HCNG fueled spark-ignition (SI) engine with its effects on performance and emissions. *Renew. Sustain. Energy Rev.* **2018**, *82*, 324–342. [CrossRef]

16. Amirante, R.; Distaso, E.; Di Iorio, S.; Sementa, P.; Tamburrano, P.; Vaglieco, B.; Reitz, R. Effects of natural gas composition on performance and regulated, greenhouse gas and particulate emissions in spark-ignition engines. *Energy Convers. Manag.* **2017**, *143*, 338–347. [CrossRef]
17. Korakianitis, T.; Namasivayam, A.; Crookes, R. Natural-gas fueled spark-ignition (SI) and compression-ignition (CI) engine performance and emissions. *Prog. Energy Combust. Sci.* **2011**, *37*, 89–112. [CrossRef]
18. Paparao, J.; Murugan, S. Oxy-hydrogen gas as an alternative fuel for heat and power generation applications-A review. *Int. J. Hydrogen Energy* **2021**, *46*, 37705–37735. [CrossRef]
19. Ceviz, M.A.; Sen, A.K.; Küleri, A.K.; Öner, I.V. Engine performance, exhaust emissions, and cyclic variations in a lean-burn SI engine fueled by gasoline–hydrogen blends. *Appl. Therm. Eng.* **2012**, *36*, 314–324. [CrossRef]
20. Greenwood, J.; Erickson, P.; Hwang, J.; Jordan, E. Experimental results of hydrogen enrichment of ethanol in an ultra-lean internal combustion engine. *Int. J. Hydrogen Energy* **2014**, *39*, 12980–12990. [CrossRef]
21. Ma, F.; Wang, M.; Jiang, L.; Deng, J.; Chen, R.; Naeve, N.; Zhao, S. Performance and emission characteristics of a turbocharged spark-ignition hydrogen-enriched compressed natural gas engine under wide open throttle operating conditions. *Int. J. Hydrogen Energy* **2010**, *35*, 12502–12509. [CrossRef]
22. Ma, F.; Wang, M.; Jiang, L.; Chen, R.; Deng, J.; Naeve, N.; Zhao, S. Performance and emission characteristics of a turbocharged CNG engine fueled by hydrogen-enriched compressed natural gas with high hydrogen ratio. *Int. J. Hydrogen Energy* **2010**, *35*, 6438–6447. [CrossRef]
23. Ma, F.; Wang, Y.; Ding, S.; Jiang, L. Twenty percent hydrogen-enriched natural gas transient performance research. *Int. J. Hydrogen Energy* **2009**, *34*, 6523–6531. [CrossRef]
24. Demirbas, A. Current advances in alternative motor fuels. *Energy Explor. Exploit.* **2003**, *21*, 475–487. [CrossRef]
25. Usman, M.; Farooq, M.; Naqvi, M.; Saleem, M.W.; Hussain, J.; Naqvi, S.R.; Jahangir, S.; Usama, J.; Muhammad, H.; Idrees, S. Use of Gasoline, LPG and LPG-HHO Blend in SI Engine: A Comparative Performance for Emission Control and Sustainable Environment. *Processes* **2020**, *8*, 74. [CrossRef]
26. Santilli, R.M. A new gaseous and combustible form of water. *Int. J. Hydrogen Energy* **2006**, *31*, 1113–1128. [CrossRef]
27. Yilmaz, A.C.; Uludamar, E.; Aydin, K. Effect of hydroxy (HHO) gas addition on performance and exhaust emissions in compression ignition engines. *Int. J. Hydrogen Energy* **2010**, *35*, 11366–11372. [CrossRef]
28. Wang, S.; Ji, C.; Zhang, J.; Zhang, B. Improving the performance of a gasoline engine with the addition of hydrogen–oxygen mixtures. *Int. J. Hydrogen Energy* **2011**, *36*, 11164–11173. [CrossRef]
29. Ji, C.; Wang, S. Effect of hydrogen addition on combustion and emissions performance of a spark ignition gasoline engine at lean conditions. *Int. J. Hydrogen Energy* **2009**, *34*, 7823–7834. [CrossRef]
30. Wang, S.; Ji, C.; Zhang, B. Starting a spark-ignited engine with the gasoline–hydrogen mixture. *Int. J. Hydrogen Energy* **2011**, *36*, 4461–4468. [CrossRef]
31. Usman, M.; Hayat, N. Use of CNG and Hi-octane gasoline in SI engine: A comparative study of performance, emission, and lubrication oil deterioration. *Energy Sources Part A Recovery Util. Environ. Eff.* **2019**, 1–15. [CrossRef]
32. Usman, M.; Hayat, N.; Bhutta, M.M.A. SI engine fueled with gasoline, CNG and CNG-HHO blend: Comparative evaluation of performance, emission and lubrication oil deterioration. *J. Therm. Sci.* **2021**, *30*, 1199–1211. [CrossRef]
33. Musmar, S.E.A.; Al-Rousan, A.A. Effect of HHO gas on combustion emissions in gasoline engines. *Fuel* **2011**, *90*, 3066–3070. [CrossRef]
34. Farooq, M.S.; Ali, U.; Farid, M.M.; Mukhtar, T. Experimental Investigation of Performance and Emissions of Spark Ignition Engine Fueled with Blends of HHO Gas with Gasoline and CNG. *Int. J. Therm. Environ. Eng.* **2021**, *18*, 27–34.
35. Wang, S.; Ji, C.; Zhang, B.; Liu, X. Performance of a hydroxygen-blended gasoline engine at different hydrogen volume fractions in the hydroxygen. *Int. J. Hydrogen Energy* **2012**, *37*, 13209–13218. [CrossRef]
36. Subramanian, B.; Ismail, S. Production and use of HHO gas in IC engines. *Int. J. Hydrogen Energy* **2018**, *43*, 7140–7154. [CrossRef]
37. EL-Kassaby, M.M.; Eldrainy, Y.A.; Khidr, M.E.; Khidr, K.I. Effect of hydroxy (HHO) gas addition on gasoline engine performance and emissions. *Alex. Eng. J.* **2016**, *55*, 243–251. [CrossRef]
38. Anwar, M.N.; Fayyaz, A.; Sohail, N.F.; Khokhar, M.F.; Baqar, M.; Khan, W.D.; Rasool, K.; Rehan, M.; Nizami, A.S. CO₂ capture and storage: A way forward for sustainable environment. *J. Environ. Manag.* **2018**, *226*, 131–144. [CrossRef]
39. Caliskan, H. Environmental and enviroeconomic researches on diesel engines with diesel and biodiesel fuels. *J. Clean. Prod.* **2017**, *154*, 125–129. [CrossRef]
40. Gürbüz, H.; Şöhret, Y.; Akçay, H. Environmental and enviroeconomic assessment of an LPG fueled SI engine at partial load. *J. Environ. Manag.* **2019**, *241*, 631–636. [CrossRef]
41. Shamekhi, A.H.; KHATIB, Z.N.; Shamekhi, A. A Comprehensive Comparative Investigation of Compressed Natural Gas as an Alternative Fuel in a Bi-fuel Spark Ignition Engine. 2008, Volume 27, pp. 73–83. Available online: <https://www.sid.ir/paper/567589/en> (accessed on 31 August 2021).
42. Ma, F.; Wang, Y.; Liu, H.; Li, Y.; Wang, J.; Zhao, S. Experimental study on thermal efficiency and emission characteristics of a lean burn hydrogen enriched natural gas engine. *Int. J. Hydrogen Energy* **2007**, *32*, 5067–5075. [CrossRef]
43. Darade, P.; Dalu, R. Investigation of performance and emissions of CNG fuelled VCR engine. *Emerg. Technol. Adv. Eng.* **2013**, *3*, 77–83.

44. Jahirul, M.I.; Masjuki, H.H.; Saidur, R.; Kalam, M.; Jayed, M.; Wazed, M. Comparative engine performance and emission analysis of CNG and gasoline in a retrofitted car engine. *Appl. Therm. Eng.* **2010**, *30*, 2219–2226. [[CrossRef](#)]
45. Duc, K.N.; Duy, V.N.; Hoang-Dinh, L.; Viet, T.N.; Le-Anh, T. Performance and emission characteristics of a port fuel injected, spark ignition engine fueled by compressed natural gas. *Sustain. Energy Technol. Assess.* **2019**, *31*, 383–389.
46. Usman, M.; Hayat, N. Lubrication, emissions, and performance analyses of LPG and petrol in a motorbike engine: A comparative study. *J. Chin. Inst. Eng.* **2020**, *43*, 47–57. [[CrossRef](#)]
47. Tang, C.F.; Tan, B.W. The impact of energy consumption, income and foreign direct investment on carbon dioxide emissions in Vietnam. *Energy* **2015**, *79*, 447–454. [[CrossRef](#)]
48. Ma, F.; Ding, S.; Wang, Y.; Wang, M.; Jiang, L.; Naeve, N.; Zhao, S. Performance and emission characteristics of a spark-ignition (SI) hydrogen-enriched compressed natural gas (HCNG) engine under various operating conditions including idle conditions. *Energy Fuels* **2009**, *23*, 3113–3118. [[CrossRef](#)]
49. Wang, Y.; Zhang, X.; Li, C.; Wu, J. Experimental and modeling study of performance and emissions of SI engine fueled by natural gas–hydrogen mixtures. *Int. J. Hydrogen Energy* **2010**, *35*, 2680–2683. [[CrossRef](#)]
50. Yan, F.; Xu, L.; Wang, Y. Application of hydrogen enriched natural gas in spark ignition IC engines: From fundamental fuel properties to engine performances and emissions. *Renew. Energy Rev.* **2018**, *82*, 1457–1488. [[CrossRef](#)]
51. Zylka, A.; Krzywanski, J.; Czakiert, T.; Idziak, K.; Sosnowski, M.; Grabowska, K.; Prauzner, T.; Nowak, W. The 4th Generation of CeSFaMB in numerical simulations for CuO-based oxygen carrier in CLC system. *Fuel* **2019**, *255*, 115776. [[CrossRef](#)]
52. Idziak, K.; Czakiert, T.; Krzywanski, J.; Zylka, A.; Kozłowska, M.; Nowak, W. Safety and environmental reasons for the use of Ni-, Co-, Cu-, Mn- and Fe-based oxygen carriers in CLC/CLOU applications: An overview. *Fuel* **2020**, *268*, 117245. [[CrossRef](#)]
53. Czakiert, T.; Krzywanski, J.; Zylka, A.; Nowak, W. Chemical looping combustion: A brief overview. *Energies* **2022**, *15*, 1563. [[CrossRef](#)]
54. Krzywanski, J.; Czakiert, T.; Nowak, W.; Shimizu, T.; Zylka, A.; Idziak, K.; Sosnowski, M.; Grabowska, K. Gaseous emissions from advanced CLC and oxyfuel fluidized bed combustion of coal and biomass in a complex geometry facility: A comprehensive model. *Energy* **2022**, *251*, 123896. [[CrossRef](#)]
55. Muhammad Ashraf, W.; Moeen Uddin, G.; Muhammad Arafat, S.; Afghan, S.; Hassan Kamal, A.; Asim, M.; Haider Khan, M.; Waqas Rafique, M.; Naumann, U.; Niazi, S.G. Optimization of a 660 MWe supercritical power plant performance—A case of industry 4.0 in the data-driven operational management Part 1. Thermal efficiency. *Energies* **2020**, *13*, 5592. [[CrossRef](#)]
56. Muhammad Ashraf, W.; Moeen Uddin, G.; Hassan Kamal, A.; Haider Khan, M.; Khan, A.A.; Afroze Ahmad, H.; Ahmed, F.; Hafeez, N.; Muhammad Zawar Sami, R.; Muhammad Arafat, S. Optimization of a 660 MWe supercritical power plant performance—A case of Industry 4.0 in the data-driven operational management. Part 2. Power generation. *Energies* **2020**, *13*, 5619. [[CrossRef](#)]
57. Sztékler, K.; Kalawa, W.; Mika, L.; Krzywanski, J.; Grabowska, K.; Sosnowski, M.; Nowak, W.; Siwek, T.; Bieniek, A. Modeling of a combined cycle gas turbine integrated with an adsorption chiller. *Energies* **2020**, *13*, 515. [[CrossRef](#)]
58. Weber, R.; Mueller, C.; Reinhart, C. Building for Zero, The Grand Challenge of Architecture without Carbon (October 8, 2021). 2021. Available online: https://papers.ssrn.com/sol3/papers.cfm?abstract_id=3939009 (accessed on 4 November 2021).
59. Yontar, A.A.; Doğu, Y. Investigation of the effects of gasoline and CNG fuels on a dual sequential ignition engine at low and high load conditions. *Fuel* **2018**, *232*, 114–123. [[CrossRef](#)]
60. Yao, Z.; Cao, X.; Shen, X.; Zhang, Y.; Wang, X.; He, K. On-road emission characteristics of CNG-fueled bi-fuel taxis. *Atmos. Environ.* **2014**, *94*, 198–204. [[CrossRef](#)]